Journal of Nanostructure in Chemistry (2019) 9:141–152
https://doi.org/10.1007/s40097-019-0304-y

ORIGINAL RESEARCH

Application of microwave irradiation for fabrication of sulfated ZrO_2–Al_2O_3 nanocomposite via combustion method for esterification reaction: process condition evaluation

Hamed Nayebzadeh[1] · Naser Saghatoleslami[2] · Mohammad Tabasizadeh[3]

Received: 17 January 2019 / Accepted: 14 May 2019 / Published online: 22 May 2019

Abstract

The zirconia–alumina nanocatalyst was prepared using microwave combustion method, and the effects of alumina/zirconia ratio, fuel-to-oxidizer ratio, and calcination temperature on its structural and chemical performance were examined. Furthermore, the most suitable synthesized nanocatalyst was impregnated using different dosages of sulfate group to improve the activity of the sample for the esterification reaction. The results revealed that there was a significant improvement in the crystalline structure of alumina and zirconia for the samples having the alumina/zirconia ratio of 2. It was also noted that some amorphous structures were observed for low fuel dosages, while the activity of the sample was reduced with higher fuel consumption than the stoichiometric ratio, which can be attributed to the increase in the crystallite size and formation of different alumina phases. Based on calcination results, non-considerable changes were observed in the morphology and activity of the catalyst. It can be concluded that the solution combustion method is suitable for nanocatalyst preparation without any requirement of further thermal treatment. In addition, the activity of the sample was enhanced by impregnation with H_2SO_4 where the conversion of 91.6% was achieved. The catalyst showed high reusability at least for seven times as well as high stability of zirconia–alumina as a support.

✉ Hamed Nayebzadeh
h.nayebzadeh@yahoo.com; h.nayebzadeh@esfarayen.ac.ir

[1] Esfarayen University of Technology, Esfarayen, North Khorasan, Iran

[2] Department of Petroleum Engineering, Eqbal Institute of Higher Education, Mashhad, Iran

[3] Department of Biosystems Engineering, Faculty of Agriculture, Ferdowsi University of Mashhad, Mashhad, Iran

Graphical abstract

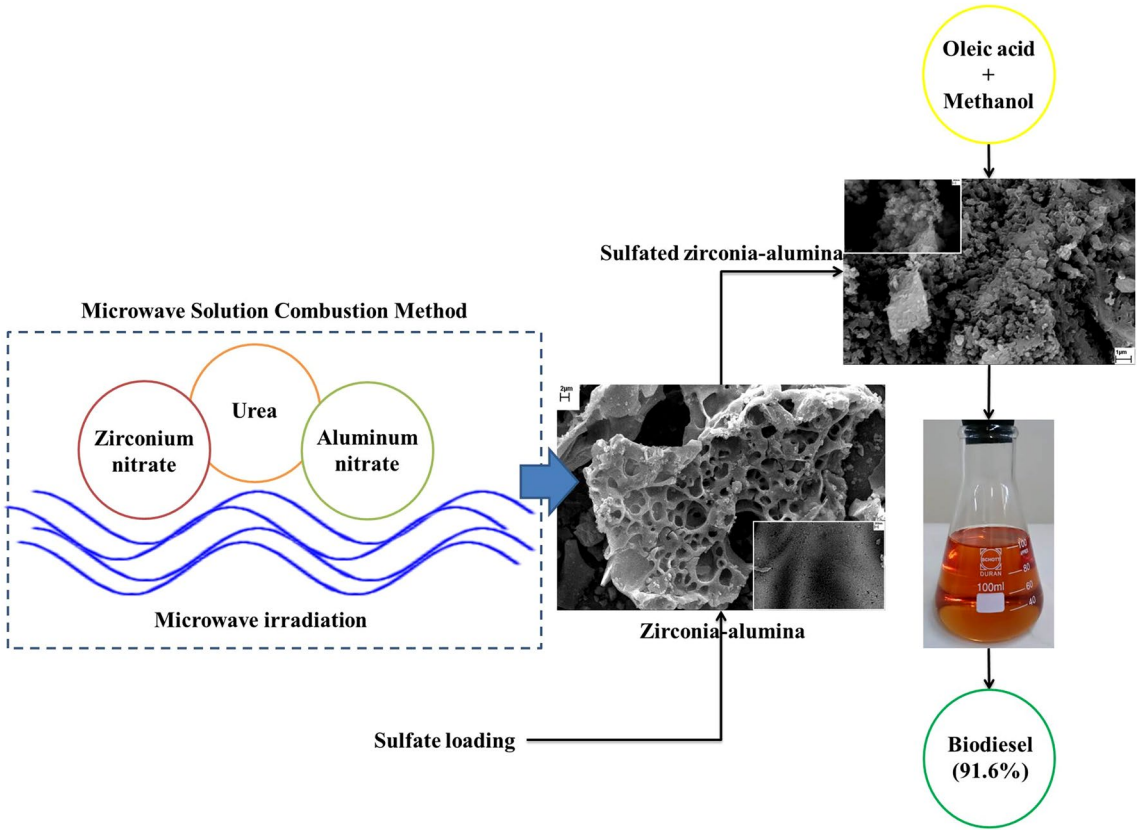

Keywords Heterogeneous catalyst · Microwave combustion method · Alumina–zirconia composite · Biodiesel · Esterification

Introduction

In the past decade, scientists have searched for an alternative to fossil fuels due to their environmental impacts, limited resources, and considerable increase in price. Biodiesel fuel is one of these alternative fossil fuels, produced from several edible and non-edible oils sources via transesterification reaction [1]. Moreover, the esterification reaction is an essential step in the production of biodiesel from waste oils and greases, usually containing high free fatty acid (FFA) contents. In these processes, homogeneous or heterogeneous catalysts must be utilized for the production of biodiesel [2].

In recent years, heterogeneous catalysts have attracted considerable attention due to the problems associated with homogeneous catalysts. Heterogeneous catalysts have numerous advantages, such as simple separation from the product, less sensitivity to FFA, ability to be recycled several times, and being environmentally friendly, waste-free, non-corrosive, and non-toxic. The heterogeneous catalysts are categorized into solid acid, solid base, and enzymatic catalysts [3]. Enzymatic catalysts take a longer time for the conversion of feedstock to biodiesel. Although solid acid catalysts have lower activities than those on solid bases, they have higher stability and can, therefore, be utilized for feedstock with large amounts of FFAs [4].

From among the solid acid catalysts, alumina and zirconia have been found to be exceptional super-catalysts for various organic transformations due to their high chemical corrosion resistance and thermal stability [5]. Moreover, researchers have reported that sulfate ions are an attractive group for the improvement of the acidity and activity of the catalysts. Therefore, several studies have been conducted on sulfated zirconia (SZ) for the production of biodiesel [6–8]. However, SZ is easily deactivated by losing sulfur groups [9, 10]. Although some researchers have reported that supporting SZ by transition metals can substantially enhance the performance of the catalyst,

serious concerns still remain about its long-term stability and/or regenerability [11, 12].

In recent years, alumina as another active and stable catalyst has been reinforced on SZ, and sulfated zirconia alumina (SZA) has been utilized for reactions such as the isomerization of n-butane [13, 14]. However, few studies have been conducted on SZA activity in the production of biodiesel. Yee et al. [15] performed extensive studies on SZA for the transesterification of palm oil with methanol into fatty acid methyl ester (FAME) in which an 83.3% yield was obtained. In another study, they also optimized the preparation conditions of SZA such as calcination temperature and time [16, 17]. Furthermore, the effect of calcination temperature and optimum amount of Al on the SZ used in esterification and transesterification reactions was evaluated in our previous works [11, 18]. In all these studies, SZA was prepared using the solvent-free method (SFM), which is a mechanical procedure for the synthesis of catalysts. It is thus concluded that SFM is not a proper method for catalyst production since it leaves large amounts of sulfate ions in the product mixture and possesses low reusability characteristics.

Several methods such as milling [19], liquid precursor methods, hydrothermal, precipitation, impregnation and sol–gel [20–22], and solution combustion method (SCM) [23, 24] have been reported for the preparation of nano-materials. However, all these techniques, except for SCM, either require high temperatures or long processing times. On the other hand, SCM is an appropriate route in terms of energy consumption, production rate, processing cost, and time-saving. SCM is a simple method in which a solution containing salts of the desired metals (usually nitrates) and fuel (commonly urea) is continuously heated to start the combustion reaction. The synthesized powder commonly has a large surface area due to the resale of large amounts of smoke during the combustion process.

Based on the reported advantages of SZA nanocatalyst and combustion method, some catalysts containing Zr/Al-mixed oxides were prepared using the SCM method in which the proportion of Al to Zr (molar ratios) was used. Moreover, the effect of fuel-to-oxidizer ratio as an important parameter in the SCM was investigated for the fabrication of high-crystalline powder along with calcination temperature for the assessment of the quality of combustion route to decompose raw materials. Finally, the best nanocatalyst synthesized via SCM at the optimized conditions was impregnated by sulfuric acid at different concentrations. In all steps, the activity of samples was evaluated by the esterification reaction of oleic acid (OA) with methanol, and the stability of the sample with the highest activity was assessed.

Experimental procedures

Preparation of zirconia–alumina nanocatalysts

For the synthesis of the zirconia–alumina nanocatalyst via SCM, microwave irradiation was utilized as the heating source due to its advantages such as reaction rate acceleration, generation of heat within the material, uniform distribution of heat, localized heating, and molecular agitation. To synthesize Zr/Al-catalysts via MCM, $ZrO(NO_3)_2{\cdot}6H_2O$ and $Al(NO_3)_3{\cdot}9H_2O$ with different molar ratios of Al_2O_3 to ZrO_2 (0.5, 1, 1.5, 2, 2.5, and 3) were dissolved in distilled water and then heated on a hot plate at 80 °C. After that, a desirable amount of urea, calculated based on the total oxidizing and reducing valences of the components for obtaining the fuel-to-oxidizer ratio, was added to the solution. The valences of the components were chosen as directed by Manikandan et al. [25]. Therefore, the oxidizing and the reducing valences of aluminum nitrate nonahydrate, zirconyl nitrate hexahydrate, and urea were obtained as −15, −10, and +6, respectively. The corresponding chemical reaction of metal nitrates and urea is shown below:

$$\begin{aligned}&(2+y)\mathrm{Al}\left(\mathrm{NO_3}\right)_3\cdot 9\mathrm{H_2O}+\mathrm{ZrO}\left(\mathrm{NO_3}\right)_2\cdot 6\mathrm{H_2O}\\&\quad+(6.67+2.5y)\mathrm{CO}\left(\mathrm{NH_2}\right)_2\rightarrow \mathrm{ZrO_2}-\mathrm{Al_2O_3}\\&\quad+(37.34+14y)\mathrm{H_2O}+(6.67+2.5y)\mathrm{CO_2}\\&\quad+(10.67+4y)\mathrm{N_2},\quad (y=-1,\ 0,\ 1,\ 2,\ 3\ \text{and}\ 4).\end{aligned}\tag{1}$$

After preparation of the clear gel, it was heated in a microwave oven (Daewoo, Model No. KOC9N2TB, microwave 900 W, and microwave frequency 2.45 GHz) at high power for 10 min. After evaporation of the remaining moisture, a high amount of smoke was released. At the point of spontaneous combustion, the exothermic reaction occurred and a white foamy catalyst was produced. The samples were labeled as ZA-0.5, ZA-1, ZA-1.5, ZA-2, ZA-2.5 and ZA-3, corresponding to the Al/Zr ratios of 0.5, 1, 1.5, 2, 2.5 and 3, respectively.

To assess the effect of fuel amount on the combustion reaction temperature and duration, the amount of fuel was changed on two levels as a lean and rich fuel. The possible combustion reaction which could occur for ZA-2 is shown as follows:

$$\begin{aligned}&4\mathrm{Al}\left(\mathrm{NO_3}\right)_3\cdot 9\mathrm{H_2O}+\mathrm{ZrO}\left(\mathrm{NO_3}\right)_2\cdot 6\mathrm{H_2O}\\&\quad+\phi(11.67)\mathrm{CO}\left(\mathrm{NH_2}\right)_2\rightarrow \mathrm{ZrO_2}-2\mathrm{Al_2O_3}\\&\quad+(42+23.34\varphi)\mathrm{H_2O}+11.67\varphi\mathrm{CO_2}\\&\quad+(7+11.67\varphi)\mathrm{N_2},\quad (\phi=0.5,\ 1\ \text{and}\ 1.5).\end{aligned}\tag{2}$$

The post-thermal treatment was used to ensure the complete decomposition of precursors to their oxides. For this purpose, the best catalyst synthesized from previous steps was calcined at different temperatures (400, 500, 600, 700, and 900 °C), respectively, labeled as ZA-2-400, ZA-2-500, ZA-2-600,

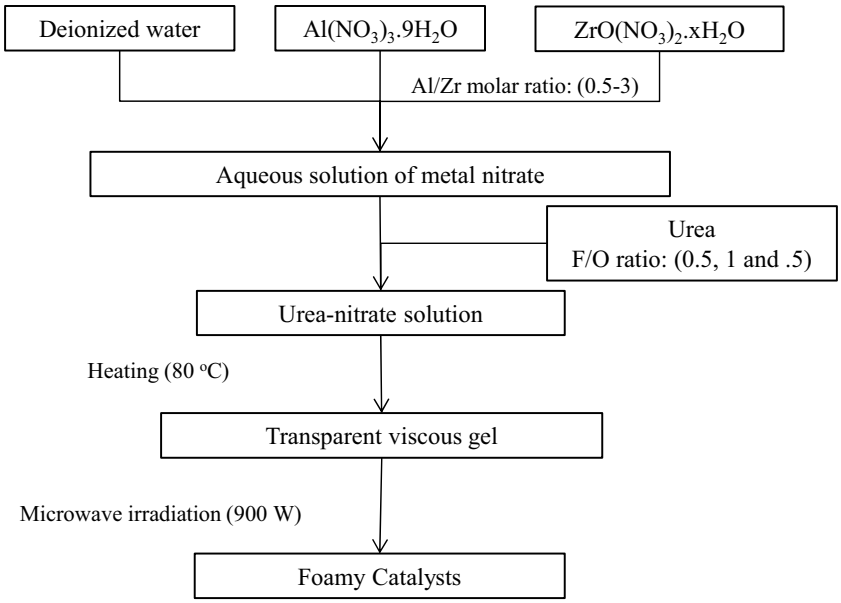

Fig. 1 Preparation of zirconia–alumina nanocatalysts via microwave combustion method (MCM)

ZA-2-700, and ZA-2-900. Figure 1 depicts the zirconia–alumina nanocatalyst fabrication methodology.

Preparation of zirconia–alumina supported by sulfate groups

The nanocatalyst obtained from the aforementioned procedure was then impregnated using different amounts of sulfate groups. To this end, 1 g of ZA-2 as the best nanocatalyst was refluxed by 10 mL of H_2SO_4 with different molarities (0.5, 1, and 2 M) at 80 °C for 2 h. Then the slurry mixture was dried in an oven at 110 °C overnight and calcined in air at 550 °C for 4 h to obtain the proper catalyst, as shown in Fig. 2.

Catalyst characterization

Phase identification and crystalline size of samples were determined by X-ray powder diffraction (UNISANTIS/XMP 300) using Cu K_α radiation at 45 kV and 80 mA, over a 2θ range from 20° to 70°. The specific surface area, mesoporous volume and mean pore size were determined by N_2 adsorption–desorption at − 196 °C using Belsorp mini II (BelJapan) system, and the evaluations were made using the BET (Brunauer–Emmett–Teller) and the BJH (Barrett–Joyner–Hollander) methods, respectively. The stretching mode frequencies of the synthesized catalysts were evaluated by Fourier-transform infrared (FTIR) technique which is used to obtain an infrared spectrum of the absorption of a catalyst in the range of 400–4000 cm^{-1}, using AVATAR 370 (Thermo Nicolet) spectrometer. The morphology and composition of the calcined catalysts at different temperatures were examined by scanning electron microscopy (SEM, LEO 1450 VP, Germany). The SEM was used in conjunction with energy-dispersive spectroscopy (EDS) to examine the purity and elemental composition of the final product. Transmission electron microscopy (TEM, Leo 912 AB, Germany) was also employed to access the particle distribution of the impregnated catalyst by sulfate groups.

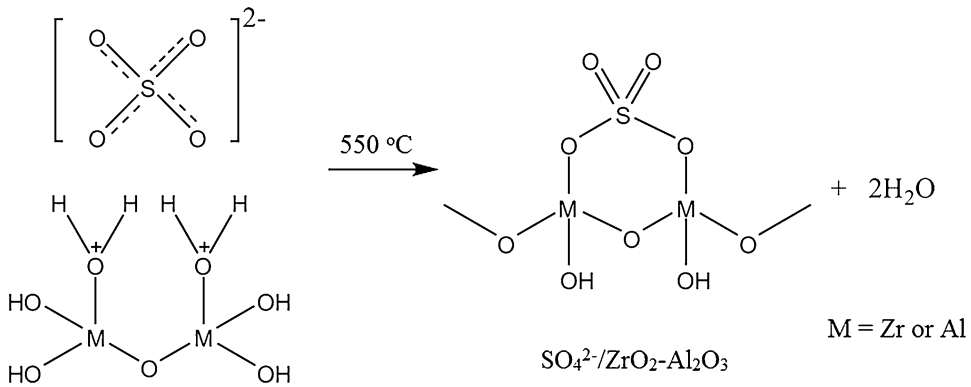

Fig. 2 Illustration of chemical reactions between metal cations and sulfate ions involved in the preparation of acidic nanocatalyst

Esterification reaction

In this study, the activity of the catalysts was investigated by means of the esterification of OA as free fatty acid with methanol. Esterification reactions were performed under batch reaction conditions using an 80-mL stainless steel reactor with a thermometer (Type K) and a barometer. The reaction was performed at 150° for the catalysts without sulfate groups due to their lower activity and at lower temperatures for sulfated catalyst [10, 11]. The other conditions were set as 9 molar ratio of fatty acid to methanol, 4 h reaction time, and 3 weight percent (wt%) of the catalyst. After the reaction and separation of the ester layer, the conversion was obtained via the standard titration method using potassium hydroxide in accordance with the reduction of the acid index of OA after the reaction.

Results and discussion

Effect of Al/Zr ratios on the properties and activity of zirconia–alumina catalyst

The XRD patterns of the samples with different Al/Zr ratios are illustrated in Fig. 3. The α-Al_2O_3 (alpha phases of alumina) and t-ZrO_2 (tetragonal phases of zirconia) were the main phases of the samples. The peaks at $2\theta = 25.5°$, 35.1°, 37.8°, 43.3°, 52.5°, 57.5°, 61.2°, 66.5°, and 68.2° were associated with the [012], [104], [110], [113], [024], [116], [211], [214], and [300] planes of α-Al_2O_3, respectively (JCPDS No. 42-1468). Moreover, the peaks at $2\theta = 30.2°$, 34.5°, 50.3°, and 60.1° corresponded to the tetragonal phases of zirconia and the monoclinic phases of zirconia (*m*-ZrO_2) observed at 24.2°, 28.2°, 31.5°, and 49.6° (JCPDS No. 84-1449). The stable alpha phase of alumina and the monoclinic phase of zirconia were formed at a higher temperature, confirming that the combustion reaction is highly exothermic [26, 27].

According to Fig. 3a, some monoclinic phases of zirconia were formed from the transition of tetragonal to monoclinic phases since the reaction temperature was not high during the preparation of ZA-0.5. It has also been earlier concluded that a lower enthalpy of zirconia formation as compared to alumina causes a lower adiabatic flame temperature which prevents the transformation of all gamma-alumina to alpha phases. Therefore, the diffraction peak of gamma-alumina was observed in the ZA-0.5 pattern. Phase transformations in the crystallization sequence of alumina and in connection with the process temperature are as follows: bayerite → boehmite → γ-alumina → δ-alumina → θ-alumina → α-alumina [28].

The ZA composite (Fig. 3b) demonstrated a less crystal structure due to the incomplete combustion process.

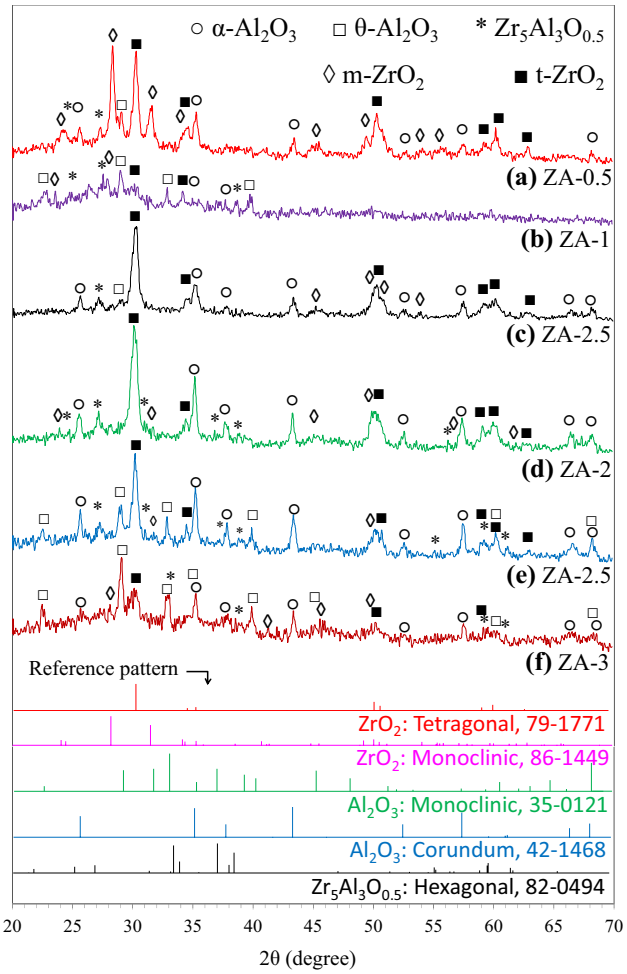

Fig. 3 XRD pattern of zirconia–alumina composite fabricated by different Zr/Al molar ratio (**a** ZA-0.5, **b** ZA-1, **c** ZA-1.5, **d** ZA-2, **e** ZA-2.5 and **f** ZA-3 nanocatalyst) via microwave combustion method

Many researchers have utilized thermal annealing (i.e., over 1000 °C) or excess fuel for the synthesis of the crystalline structure of the ZA composite [29]. The crystalline structure of alumina and zirconia was primarily arranged for higher loading of alumina, as depicted in Fig. 3c. It may be for the high combustion enthalpy of aluminum nitrate which enhances the temperature of reaction during combustion. Furthermore, the zirconia phase retained its tetragonal forms for all samples with Al/Zr ratios greater than 1. It can also be concluded that, with increasing the amount of alumina to twice the amount of stoichiometric ratio (ZA-2), the high-crystalline phases of α-Al_2O_3 and *t*-ZrO_2 with relatively extended peaks would be observed. Moreover, the peaks become narrower and sharper with the increase of alumina cations. Figure 3f demonstrates that the increase in alumina cations resulted in the formation of alumina phases (i.e., gamma, theta, and alpha), probably due to the poor distribution of heat during the preparation of the catalyst.

Table 1 Physicochemical properties of zirconia–alumina nanocomposite fabricated by microwave combustion method

Catalyst	Al/Zr mole ratio	Crystalline size using XRD (nm)		BET surface area ($m^2\ g^{-1}$)	Pore volume ($cm^3\ g^{-1}$)	Pore size (nm)	Yield (%)
		Al_2O_3	ZrO_2				
ZA-0.5	0.5	15	16.5	–	–	–	67.1
ZA-1	1	–	–	3.71	0.0067	3.8	70.7
ZA-1.5	1.5	15.5	14	8.22	0.0090	4.2	73.3
ZA-2	2	16	12	14.35	0.0017	4.9	79.2
ZA-2.5	2.5	17.5	13	9.10	0.0077	3.1	71.4
ZA-3	3	17	14	–	–	–	58.6
ZR-2L	2	17	–	–	–	–	43.7
ZR-2R	2	20	15	–	–	–	65.4

Reaction conditions: 150 °C, 9 molar ratios of methanol/OA, 3 wt% of catalyst and for a period of 4 h

Scherer's equation was used to calculate the crystallite size of the samples as listed in Table 1. The samples fabricated at Zr/Al ratios greater than 1 presented a similar crystalline size, whereas the ZA-2 nanocatalyst exhibited almost the lowest zirconia and alumina crystals size. Researchers have reported the effect of crystallite size on the performance of the catalyst in the biodiesel production process [30–32].

The results of BET analysis and activity are also shown in Table 1. The results illustrate that the highest surface area providing a higher active site for the reactant interaction belongs to ZA-2. The ZA-2 nanocatalyst was able to convert 79.2% of OA into its methyl ester.

Effect of F/O ratios on the properties and activity of zirconia–alumina catalyst

Figure 4 displays the XRD patterns of synthesized ZA-2 for fuel to oxidizer ratios (F/O) of 0.5, 1, and 1.5, labeled as ZA-2L, ZA-2, and ZA-2R, respectively. Fuels must exhibit the following characteristics: ability to participate as a reduction agent and ability to act as a source of energy in the SCM. Therefore, for the F/O ratio of 0.5 (Fig. 4a), the low temperature of the catalyst synthesis medium resulted by the incomplete combustion reaction led to no peaks for zirconia, and alpha-alumina was detected [24, 33].

Increasing the F/O ratio from 0.5 to 1.0 resulted in the increase of reaction temperature and duration, thereby causing the formation of zirconia and alpha-alumina. Since the key elements in urea are C and H, the higher amounts of fuel will reinforce the reduction in the potential of the solution and the main oxide peaks' changes from the gamma and theta of alumina to the alpha phases (Fig. 4b) [34]. Figure 4c also demonstrates an increase in the intensity of α-alumina and *t*-ZrO_2 when an excess amount of fuel was used [35, 36].

Based on Scherer's equation (see Table 1), an increase in the F/O ratio from 1 to 1.5 resulted in the increase of the crystallite size of alumina and *t*-ZrO_2. This can be related to

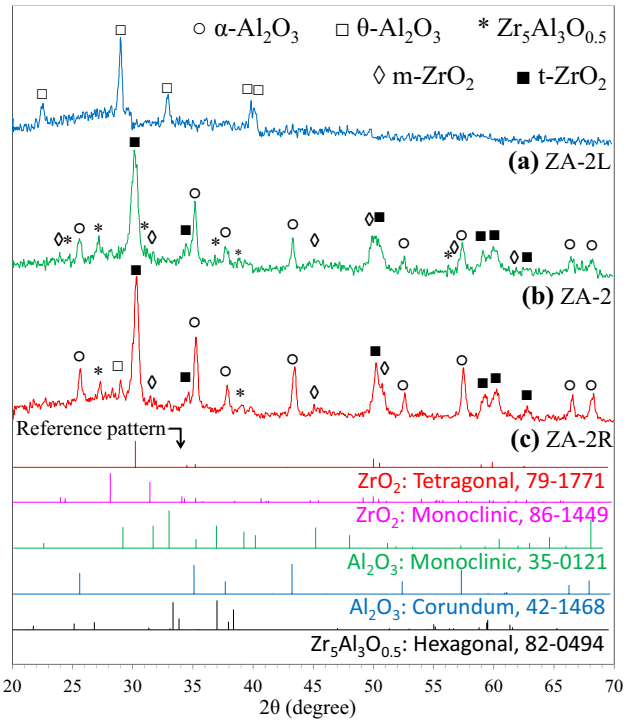

Fig. 4 XRD pattern of zirconia–alumina composite fabricated by Zr/Al molar ratio of 2 via microwave combustion method at different fuel-to-oxidizer (F/O) ratio (**a** ZA-2L, **b** ZA-2 and **c** ZA-2R)

the increase in combustion temperature and duration during the synthesis of the catalyst that caused an increase in the crystallite size of the zirconia–alumina nanocatalyst [33, 37].

Figure 5 demonstrates the FTIR spectra of ZA-2 for different amounts of F/O ratios. Figure 5a exhibits a broad band between 400 and 750 cm^{-1}, corresponding to the vibrational frequencies of O–Al–O related to γ-alumina [11, 38]. Furthermore, the band at 828 cm^{-1} corresponds to Al–O bonds resulting from the stretching of AlO_4 [29]. The ZA-2 nanocatalyst demonstrates only α-Al_2O_3 due to the increase of the temperature during the preparation

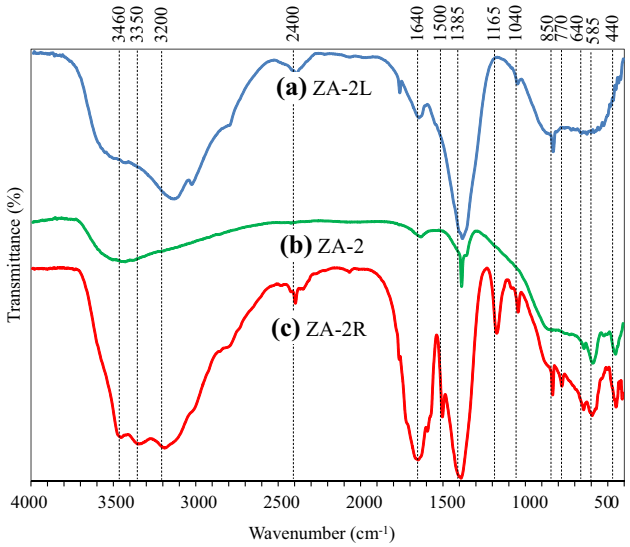

Fig. 5 FTIR spectra of zirconia–alumina composite fabricated by Zr/Al molar ratio of 2 via microwave combustion method at different fuel-to-oxidizer (F/O) ratio (**a** ZA-2L, **b** ZA-2 and **c** ZA-2R)

of the catalyst. In addition, the bands at 486, 510, 583, and 630 cm^{-1} correspond to the stretching and bending vibrations of AlO_6, and the band at 857 cm^{-1} corresponds to the stretching vibration of Al–O in AlO_4 [5, 38]. An identical spectrum in the range of 400–800 cm^{-1} was also observed for F/O ratios greater than 1. This is consistent with the fact that only octahedral Al atoms are present for the corundum structure, a result in good agreement with XRD patterns. It was also observed that the stretching vibration at 440 cm^{-1} and a weak band at 506 cm^{-1} correspond to the Zr–O vibration [26]. Furthermore, the zirconia band also appeared in the 420 cm^{-1} for ZA-2R which is an indication of the formation of more crystalline Zr–O–Zr bands [39]. Moreover, the weak bands at 520 and 545 cm^{-1} are attributed to Zr–O stretching modes [27, 40].

Figure 5 also demonstrates the stretching vibration and bending mode of O–H at about 3450 and 1643 cm^{-1} [41]. The intensity of the O–H band in the samples illustrates that the ZA-2 has less tendency to adsorb water. Furthermore, some absorption peaks for the stretching vibration of OH in the range of 3000–3600 cm^{-1} for Zr-2R and Zr-2L were also observed, corresponding to the stretching vibration of Al–OH. The bands in the vicinity of 1040, 1166 (bending vibration), and 1385 cm^{-1} (stretching vibration) also corresponded to Al–O–H groups [42, 43]. The results show that ZA-2 only shows a thin bond at 1385 cm^{-1} which corresponds to its lower hydrophobicity properties. Moreover, only ZA-2 did not show peaks at 1508 and 2340 cm^{-1} corresponding to nitrate and carbonate, which is responsible for its suitability for biomedical applications [44].

The results of esterification reaction (see Table 1) revealed that the activity of the ZA-2L catalyst in the esterification reaction was very low (only 43.7% of OA was converted to its methyl ester) due to its amorphous structure and inadequate distribution of zirconia on the surface of the catalyst. On the other hand, it was observed that activity decreased for the ZA-2R compared to ZA-2, and the yield of 65.4% was obtained.

Effect of calcination temperature on the properties and activity of zirconia–alumina catalyst

After selecting the ZA-2 nanocatalyst as the best catalyst for the esterification reaction due to its high surface area, high crystallinity, low crystalline size, and higher activity, it was calcined at 400, 500, 600, 700, and 900 °C. The post-thermal treatment can give information about the combustion reaction. The samples were, respectively, converted 77.1%, 77.3%, 77.6%, 79.0%, and 80.2% of OA to methyl oleate under the reaction conditions. The results indicated that the calcination temperature has a minor effect on the activity of the catalyst due to the little influence of calcination on the decomposition of unreacted precursors and/or transformation of crystals into active phases. It can be clearly concluded that the MCM is an appropriate route for the production of mesoporous powders with high crystallinity and surface area, whereas no further thermal treatment is required.

Figure 6 shows the SEM images of ZA-2, ZA-2-400, and ZA-2-900 catalysts. The samples have porous structures with large diameters due to huge exhausted gases during catalyst synthesis by the combustion method. The SEM image of nanocatalysts with high magnification shows that the obtained nanocatalysts have porous structures with highly uniform porosity in size and shape, such that the porosity is most uniform in the ZA-2-400 sample. With an increase in the calcination temperature to 900 °C, some zirconia crystals egress from the alumina–zirconia structure and uniformly disperse on the surface of the nanocatalyst, with particle sizes in the range of about 40–90 nm. This causes a small increase in the yield of the esterification reaction when the ZA-2-900 nanocatalyst is employed. Although there were negligible changes in the morphology of samples by increasing the calcination temperature, their activity did not significantly change, a result proving that MCM is an appropriate method for the preparation of nanocatalyst without a requirement for further thermal treatment. Therefore, the ZA-2 nanocatalyst has the best properties as either a catalyst or a support for the production of biodiesel.

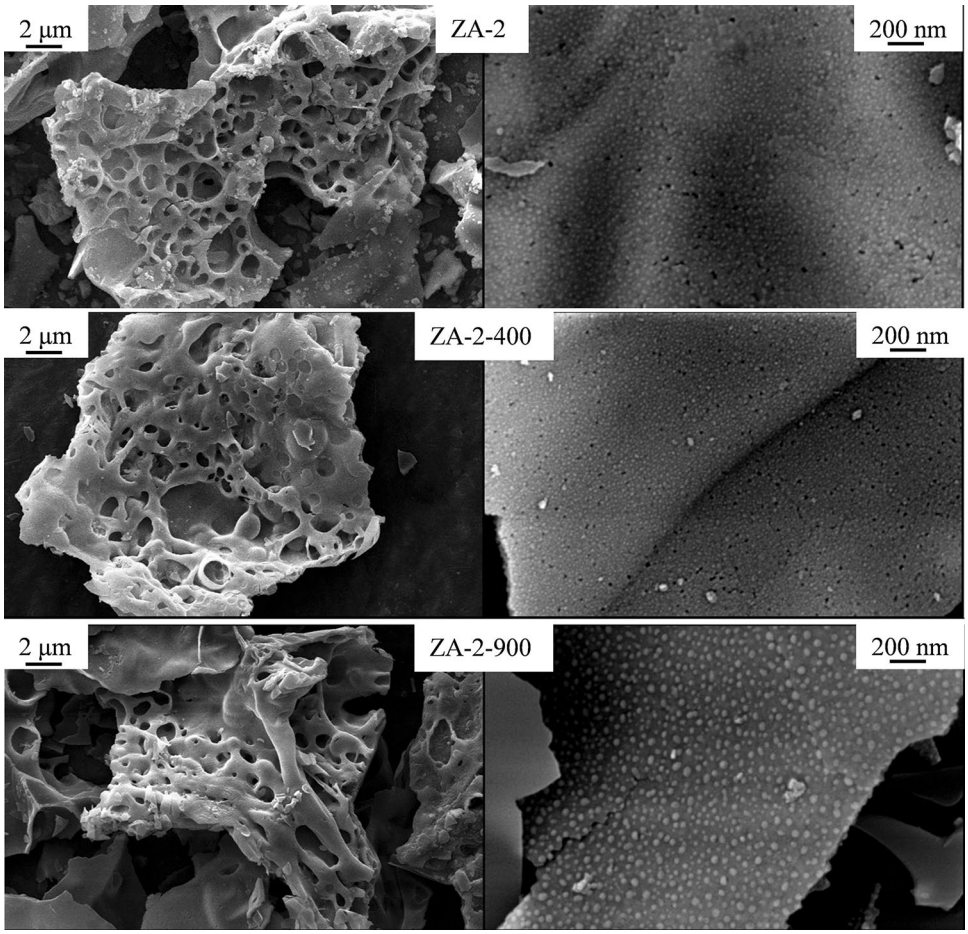

Fig. 6 SEM images of zirconia–alumina composite fabricated by Zr/Al molar ratio of 2 via microwave combustion method calcined at different temperatures

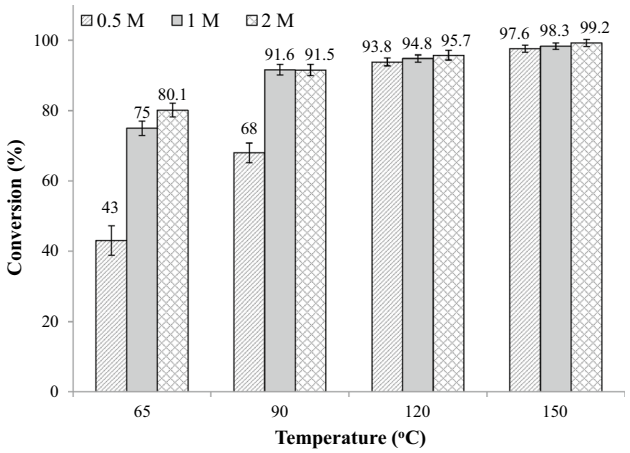

Fig. 7 Effect of sulfate content on the activity of zirconia–alumina composite fabricated by Zr/Al molar ratio of 2 via microwave combustion method used in the esterification reaction at different reaction temperatures

Effect of sulfate contents on the properties and activity of zirconia–alumina catalyst

The effect of sulfate concentration has been studied by the addition of 10 cc of H_2SO_4 with different molarities (0.5, 1, and 2 M) to 1 g of ZA-2. The activity of the sulfated catalyst was evaluated at different reaction temperatures (65, 90, 120, and 150 °C). Figure 7 shows the effect of temperature on conversion at the constant concentration of H_2SO_4. There was a steady increase in the conversion up to the maximum temperature of 120 °C, after which this increase remained constant. It is reported in the literature that an increase in temperature would accelerate the reaction rate, resulting in a significant increase in conversion efficiency [11]. Figure 7 also demonstrates that, when the concentration of H_2SO_4 was increased from 0.5 to 1 M, the conversion of OA sharply increased at lower temperatures (i.e., 65 and 90 °C) due to the enhancement of the number of active sites, while the increase of yield was not noticeable at higher temperatures (over 90 °C).

The nitrogen adsorption–desorption isotherms and pore size distribution of ZA-2 and 1S-ZA-2 nanocatalysts are illustrated in Fig. 8. Both samples show a characteristic

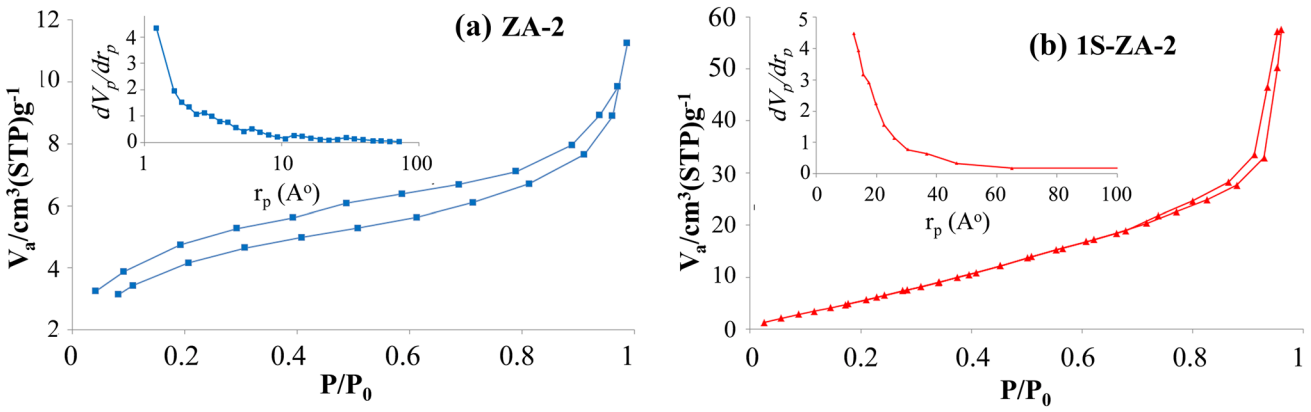

Fig. 8 Hysteresis loops of N_2 adsorption–desorption isotherm (inset: BJH pore size distribution) of zirconia–alumina composite fabricated by Zr/Al molar ratio of 2 via microwave combustion method (**a** ZA-2) and reinforced by sulfate group (**b** 1S-ZA-2)

type IV related to mesoporous materials [11]. Moreover, the hysteresis loops of the catalysts, which provide specific information about catalysts porosity, showed the H2 type usually related to mesoporous samples of complex structure, whereas H3 type hysteresis was observed for the 1S-ZA-2 nanocatalyst corresponding to the plate-like particles with slit-shaped pores [33, 41].

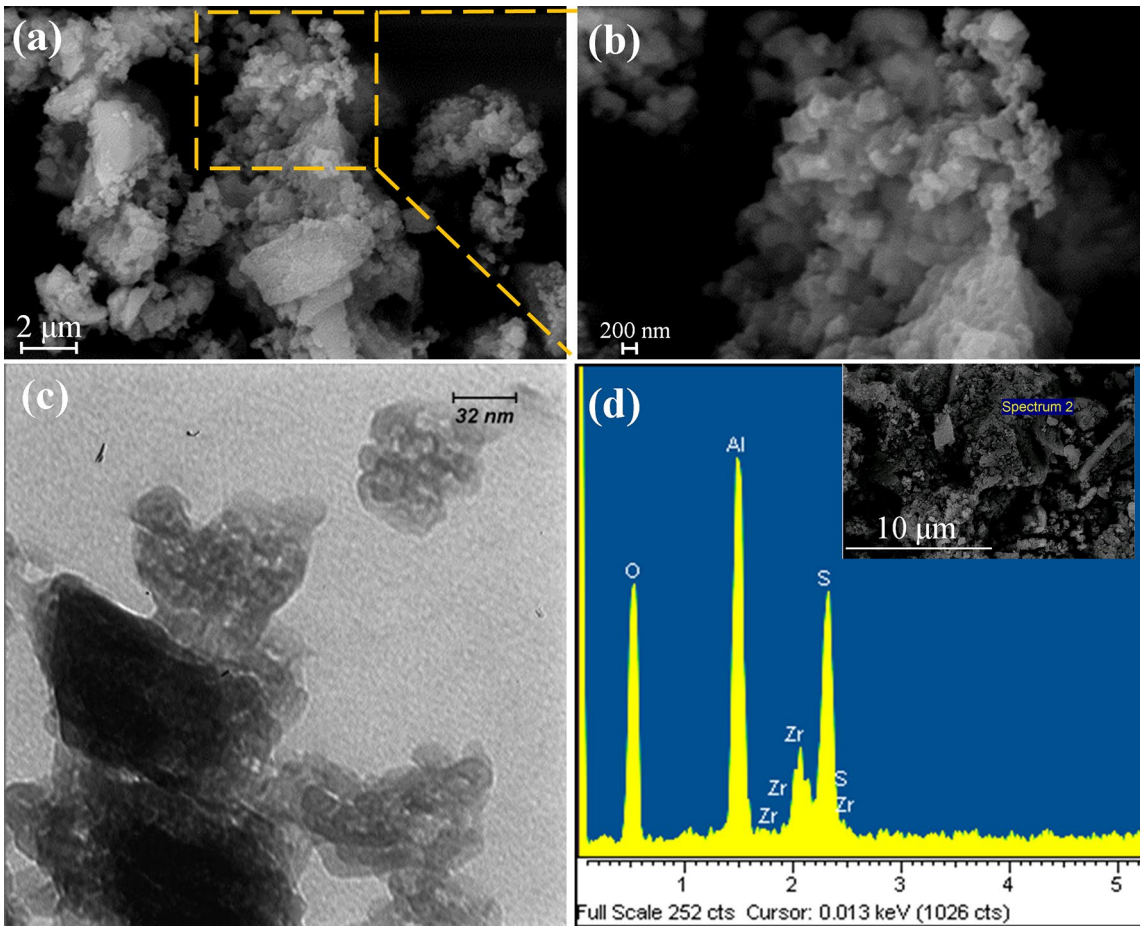

Fig. 9 **a**, **b** SEM images with different magnification, **c** TEM and **d** EDS images of sulfated zirconia–alumina composite fabricated by Zr/Al molar ratio of 2 via microwave combustion method

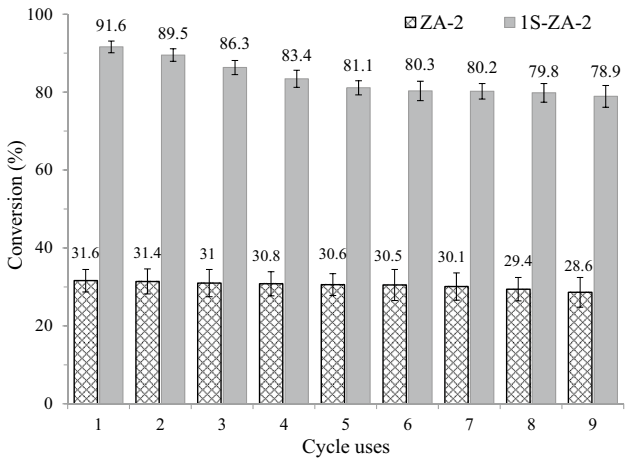

Fig. 10 Reusability of ZA-2 and 1S-ZA-2 nanocatalyst examined at the reaction conditions of 90 °C, 9 molar ratio of methanol/oleic acid, 3 wt% of catalyst and reaction time of 4 h

The pore size distribution of the samples as illustrated inside the nitrogen adsorption–desorption isotherms demonstrated insignificant changes in pore size with sulfate group loading. The catalysts presented pore diameters greater than 2 nm, classifying them as mesoporous materials [23]. Based on the BET analysis, the surface area was increased from 14.35 to 32.67 $m^2\ g^{-1}$ by sulfate group loading. It is worth noting that as the mean pore diameter was slightly decreased from 4.9 to 4.5 nm, the pore volume increased to 0.123 $cm^3\ g^{-1}$.

The SEM, TEM, and EDS images of 1S-ZA-2 are demonstrated in Fig. 9. The SEM image (Fig. 9a) illustrates that the porous structure of the 1S-ZA-2 had the tendency to form aggregates, since porosity plays an important role in the enhancement of the available active sites. The TEM image in Fig. 9b indicates that the particle size of the 1S-ZA-2 is about 50 nm and has a smooth surface as a result of modification. Furthermore, Fig. 9c exhibits the EDS spectrum of the 1S-ZA-2 and shows the presence of sulfur, aluminum, zirconium, and oxygen, while no trace of contaminated elements was observed.

Reusability of ZA-2 and 1S-ZA-2 nanocatalysts

The reusability of the 1S-ZA-2 nanocatalyst and its support (ZA-2) was evaluated as shown in Fig. 10. The catalysts were washed twice with methanol after each run, dried at 110 °C overnight, and then used. The ZA-2 and 1S-ZA-2 nanocatalysts were tested in the reaction temperatures of 90 °C. It can be clearly observed that the activity of ZA-2 nanocatalyst was maintained constant with nine uses, confirming the stability of zirconia–alumina as a support for industrial usage. In addition, the 1S-ZA-2 nanocatalyst showed a slight reduction in the conversion due to the leaching of sulfate groups on the product mixture. However, the catalytic activity of samples was maintained constant after five uses, demonstrating that the remaining sulfate groups have a strong bond with the surface of the support, and structure and morphology did not seem to change after several uses. This proves the high stability of ZA-2 and 1S-ZA-2 nanocatalysts for several uses in the esterification reaction, making them excellent catalysts for industrial applications.

Comparison with the literatures

Coutinho et al. [45] reported that the $ZnO–Al_2O_3$ synthesized by SCM can convert 5% of OA to its ester at 160 °C, 4 molar ratios of methanol to FFA, and 5 wt% of the catalyst, at the reaction time of 1 h. In other studies, sulfated alumina prepared by sol–gel method was examined in the esterification of OA and the yield of 40% was obtained under operating conditions of 90 °C, 10 molar ratios of ethanol to FFA, 5 wt% of the catalyst, and a reaction time of 6 h [46]. Some researchers studied sulfated titania and silica synthesized by impregnation and sol–gel methods [47, 48]. They evaluated the esterification of OA which resulted in a yield of 82.2% (with the operating conditions of 80 °C, 10 molar ratios of methanol to FFA, 2 wt% of the catalyst, and the reaction period of 3 h) and 95% (120 °C, 20 molar ratios of methanol to FFA, 10 wt% of the catalyst, and the reaction period of 5 h), respectively. SO_4^{2-}/Sr-Fe oxide (20 mL of 2 M H_2SO_4 per g of composite) was converted around 97% of OA to ester at the conditions of 100 °C, 10 wt% of catalyst, 4 molar ratio of methanol to oleic acid, and the reaction time of 2 h [49].

The findings of this study revealed that the prepared catalyst possessed a high activity at low esterification reaction temperatures. Furthermore, the procedure employed for catalyst preparation (i.e., MCM) was more efficient and less time consuming than those reported in the literature. The fabricated catalyst has favorable properties such as high surface area, pore diameter, and activity.

Conclusion

In the present study, mesoporous zirconia–alumina nanocatalyst was prepared using a simple eco-friendly MCM, and catalyst preparation conditions such as Al/Zr and F/O ratios were examined. The results revealed that the stoichiometric amount of alumina-to-zirconia exhibited an amorphous structure, while for the ratios greater than 1, its crystalline structures substantially increased. It was also concluded that the ZA-2 exhibited the highest surface area and the smallest crystallite size. Furthermore, the enhancement of F/O ratio resulted in an increase in the crystallite size and reduced the

activity accordingly. It was also discovered that calcination did not have any effect on the activity and morphology of the ZA-2 nanocatalyst. The sample showed high reusability for industrial application without any reduction in the activity. It was then modified by attaching a sulfate group to it to improve the acidic properties for the esterification of OA. The results revealed that the ZA-2 nanocatalyst supported by 1 M of H_2SO_4 converted over 91% of OA to its ester at the optimized operating conditions of 90 °C, 3 wt% of the catalyst, and the methanol/OA molar ratio of 9. Finally, the synthesis process was a more economically favorable, environmentally friendly, and efficient method when compared with the methods cited in the literature.

Acknowledgements The authors gratefully acknowledge the financial support of Ferdowsi University of Mashhad (Project No. 32009) and the Iran Nanotechnology Initiative Council (Project No. 80968).

References

1. Avhad, M.R., Marchetti, J.M.: Innovation in solid heterogeneous catalysis for the generation of economically viable and ecofriendly biodiesel: a review. Catal. Rev. **58**(2), 157–208 (2016)
2. Kirubakaran, M., Arul Mozhi Selvan, V.: A comprehensive review of low cost biodiesel production from waste chicken fat. Renew. Sustain. Energy Rev. **82**, 390–401 (2018)
3. Jamil, F., Al-Haj, L., Al-Muhtaseb Ala'a, H., Al-Hinai Mohab, A., Baawain, M., Rashid, U., Ahmad Mohammad, N.M.: Current scenario of catalysts for biodiesel production: a critical review. Rev. Chem. Eng. **34**(2), 267–297 (2018)
4. Wang, A., Wang, J., Lu, C., Xu, M., Lv, J., Wu, X.: Esterification for biofuel synthesis over an eco-friendly and efficient kaolinite-supported $SO_4^{2-}/ZnAl_2O_4$ macroporous solid acid catalyst. Fuel **234**, 430–440 (2018)
5. Hashemzehi, M., Saghatoleslami, N., Nayebzadeh, H.: A study on the structure and catalytic performance of $Zn_xCu_{1-x}Al_2O_4$ catalysts synthesized by the solution combustion method for the esterification reaction. C. R. Chim. **19**(8), 955–962 (2016)
6. Teixeira, C.O.P., Pedro, K.C.N.R., Fernandes, T.L.A.P., Henriques, C.A., Zotin, F.M.Z.: Esterification of high acidity vegetable oil catalyzed by tin-based catalysts with different sulfate contents: contribution of homogeneous catalysis. Chem. Eng. Commun. **206**(2), 169–181 (2019)
7. Shi, G.-L., Yu, F., Yan, X.-L., Li, R.-F.: Synthesis of tetragonal sulfated zirconia via a novel route for biodiesel production. J. Fuel Chem. Technol. **45**(3), 311–316 (2017)
8. Dehghani, S., Haghighi, M.: Sono-sulfated zirconia nanocatalyst supported on MCM-41 for biodiesel production from sunflower oil: influence of ultrasound irradiation power on catalytic properties and performance. Ultrason. Sonochem. **35**, 142–151 (2017)
9. Li, X., Tong, D., Hu, C.: Efficient production of biodiesel from both esterification and transesterification over supported SO_4^{2-}–MoO_3–ZrO_2–Nd_2O_3/SiO_2 catalysts. J. Energy Chem. **24**(4), 463–471 (2015)
10. Nayebzadeh, H., Saghatoleslami, N., Maskooki, A., Rahmani Vahid, B.: Preparation of supported nanosized sulfated zirconia by strontia and assessment of its activities in the esterification of oleic acid. Chem. Biochem. Eng. Q. **25**(3), 259–265 (2014)
11. Rahmani Vahid, B., Saghatoleslami, N., Nayebzadeh, H., Toghiani, J.: Effect of alumina loading on the properties and activity of SO_4^{2-}/ZrO_2 for biodiesel production: process optimization via response surface methodology. J. Taiwan Inst. Chem. Eng. **83**, 115–123 (2018)
12. Zhang, Y., Chen, T., Zhang, G., Wang, G., Zhang, H.: Mesoporous Al-promoted sulfated zirconia as an efficient heterogeneous catalyst to synthesize isosorbide from sorbitol. Appl. Catal. A **562**, 258–266 (2018)
13. Hwang, C.-C., Mou, C.-Y.: Alumina-promoted sulfated mesoporous zirconia catalysts. J. Phys. Chem. C **113**(13), 5212–5221 (2009)
14. Wang, J.-H., Mou, C.-Y.: Alumina-promoted mesoporous sulfated zirconia: a catalyst for *n*-butane isomerization. Appl. Catal. A **286**(1), 128–136 (2005)
15. Yee, K.F., Kansedo, J., Lee, K.T.: Biodiesel production from palm oil via heterogeneous transesterification: optimization study. Chem. Eng. Commun. **197**(12), 1597–1611 (2010)
16. Yee, K.F., Wu, J.C.S., Lee, K.T.: A green catalyst for biodiesel production from jatropha oil: optimization study. Biomass Bioenergy **35**(5), 1739–1746 (2011)
17. Yee, K.F., Lee, K.T., Abdullah, A.Z., Wu, J.C.S.: An alternative route for the preparation of sulfated zirconia loaded on alumina (SZA) for biodiesel production: an optimization study. Energy Sour. A Recov. Util. Environ. Effects **35**(14), 1296–1305 (2013)
18. Vahid, B.R., Saghatoleslami, N., Nayebzadeh, H., Maskooki, A.: Preparation of nano-size Al-promoted sulfated zirconia and the impact of calcination temperature on its catalytic activity. Chem. Biochem. Eng. Q. **26**(2), 71–77 (2012)
19. Deirmina, F., AlMangour, B., Grzesiak, D., Pellizzari, M.: H13–partially stabilized zirconia nanocomposites fabricated by high-energy mechanical milling and selective laser melting. Mater. Des. **146**, 286–297 (2018)
20. Luo, Y., Mei, Z., Liu, N., Wang, H., Han, C., He, S.: Synthesis of mesoporous sulfated zirconia nanoparticles with high surface area and their applies for biodiesel production as effective catalysts. Catal. Today **298**, 99–108 (2017)
21. Raia, R.Z., da Silva, L.S., Marcucci, S.M.P., Arroyo, P.A.: Biodiesel production from *Jatropha curcas* L. oil by simultaneous esterification and transesterification using sulphated zirconia. Catal. Today **289**, 105–114 (2017)
22. Mahdavi, M., Abedini, E., Darabi, A.H.: Biodiesel synthesis from oleic acid by nano-catalyst (ZrO_2/Al_2O_3) under high voltage conditions. RSC Adv. **5**(68), 55027–55032 (2015)
23. Nayebzadeh, H., Saghatoleslami, N., Haghighi, M., Tabasizadeh, M., Binaeian, E.: Comparative assessment of the ability of a microwave absorber nanocatalyst in the microwave-assisted biodiesel production process. C. R. Chim. **21**(7), 676–683 (2018)
24. Nayebzadeh, H., Haghighi, M., Saghatoleslami, N., Tabasizadeh, M., Yousefi, S.: Fabrication of carbonated alumina doped by calcium oxide via microwave combustion method used as nanocatalyst in biodiesel production: influence of carbon source type. Energy Convers. Manag. **171**, 566–575 (2018)
25. Manikandan, A., Vijaya, J.J., Kennedy, L.J., Bououdina, M.: Microwave combustion synthesis, structural, optical and magnetic properties of $Zn_{1-x}Sr_xFe_2O_4$ nanoparticles. Ceram. Int. **39**(5), 5909–5917 (2013)
26. Shi, G., Yu, F., Wang, Y., Pan, D., Wang, H., Li, R.: A novel one-pot synthesis of tetragonal sulfated zirconia catalyst with high

activity for biodiesel production from the transesterification of soybean oil. Renew. Energy **92**, 22–29 (2016)
27. Altass, H.M., Khder, A.E.R.S.: Surface and catalytic properties of triflic acid supported zirconia: effect of zirconia tetragonal phase. J. Mol. Catal. A Chem. **411**, 138–145 (2016)
28. Ipek, M., Zeytin, S., Bindal, C.: Effect of ZrO_2 on phase transformation of Al_2O_3. Ceram. Int. **36**(3), 1159–1163 (2010)
29. Zhang, Q., Wei, F., Ma, P., Zhang, Y., Wei, F., Chen, H.: Mesoporous Al–Mo oxides as an effective and stable catalyst for the synthesis of biodiesel from the esterification of free-fatty acids in non-edible oils. Waste Biomass Valoriz. **9**(6), 911–918 (2018)
30. Rahmani Vahid, B., Haghighi, M., Alaei, S., Toghiani, J.: Reusability enhancement of combustion synthesized $MgO/MgAl_2O_4$ nanocatalyst in biodiesel production by glow discharge plasma treatment. Energy Convers. Manag. **143**, 23–32 (2017)
31. Gardy, J., Hassanpour, A., Lai, X., Ahmed, M.H., Rehan, M.: Biodiesel production from used cooking oil using a novel surface functionalised TiO_2 nano-catalyst. Appl. Catal. B **207**, 297–310 (2017)
32. Dantas, J., Leal, E., Cornejo, D.R., Kiminami, R.H.G.A., Costa, A.C.F.M.: Biodiesel production evaluating the use and reuse of magnetic nanocatalysts $Ni_{0.5}Zn_{0.5}Fe_2O_4$ synthesized in pilot-scale. Arab. J. Chem. **12**(4), 140–150 (2018)
33. Rahmani Vahid, B., Haghighi, M.: Urea-nitrate combustion synthesis of $MgO/MgAl_2O_4$ nanocatalyst used in biodiesel production from sunflower oil: influence of fuel ratio on catalytic properties and performance. Energy Convers. Manag. **126**, 362–372 (2016)
34. Alaei, S., Haghighi, M., Toghiani, J., Rahmani Vahid, B.: Magnetic and reusable $MgO/MgFe_2O_4$ nanocatalyst for biodiesel production from sunflower oil: influence of fuel ratio in combustion synthesis on catalytic properties and performance. Ind. Crops Prod. **117**, 322–332 (2018)
35. Khoshbin, R., Haghighi, M., Margan, P.: Combustion dispersion of CuO–ZnO–Al_2O_3 nanocatalyst over HZSM-5 used in DME production as a green fuel: effect of citric acid to nitrate ratio on catalyst properties and performance. Energy Convers. Manag. **120**, 1–12 (2016)
36. Shi, Z., Gao, H., Wang, X., Li, C., Wang, W., Hong, Z., Zhi, M.: One-step synthesis of monolithic micro-nano yttria stabilized ZrO_2-Al_2O_3 composite aerogel. Microporous Mesoporous Mater. **259**, 26–32 (2018)
37. Ajamein, H., Haghighi, M.: On the microwave enhanced combustion synthesis of CuO–ZnO–Al_2O_3 nanocatalyst used in methanol steam reforming for fuel cell grade hydrogen production: effect of microwave irradiation and fuel ratio. Energy Convers. Manag. **118**, 231–242 (2016)
38. Gardy, J., Osatiashtiani, A., Céspedes, O., Hassanpour, A., Lai, X., Lee, A.F., Wilson, K., Rehan, M.: A magnetically separable SO_4/Fe-Al-TiO_2 solid acid catalyst for biodiesel production from waste cooking oil. Appl. Catal. B **234**, 268–278 (2018)
39. Sistani, A., Saghatoleslami, N., Nayebzadeh, H.: Influence of calcination temperature on the activity of mesoporous CaO/TiO_2–ZrO_2 catalyst in the esterification reaction. J. Nanostruct. Chem. **8**(3), 321–331 (2018)
40. Wang, X., Wu, Z., Zhi, M., Hong, Z.: Synthesis of high temperature resistant ZrO_2-SiO_2 composite aerogels via "thiol-ene" click reaction. J. Sol–Gel. Sci. Technol. **87**(3), 734–742 (2018)
41. Nayebzadeh, H., Saghatoleslami, N., Haghighi, M., Tabasizadeh, M.: Influence of fuel type on microwave-enhanced fabrication of KOH/$Ca_{12}Al_{14}O_{33}$ nanocatalyst for biodiesel production via microwave heating. J. Taiwan Inst. Chem. Eng. **75**, 148–155 (2017)
42. Zhang, X., Ma, Q., Cheng, B., Wang, J., Li, J., Nie, F.: Research on KOH/La-Ba-Al_2O_3 catalysts for biodiesel production via transesterification from microalgae oil. J. Nat. Gas Chem. **21**(6), 774–779 (2012)
43. Nayebzadeh, H., Haghighi, M., Saghatoleslami, N., Alaei, S., Yousefi, S.: Texture/phase evolution during plasma treatment of microwave-combustion synthesized KOH/$Ca_{12}Al_{14}O_{33}$-C nanocatalyst for reusability enhancement in conversion of canola oil to biodiesel. Renew. Energy **139**, 28–39 (2019)
44. Ghosh, S.K., Prakash, A., Datta, S., Roy, S.K., Basu, D.: Effect of fuel characteristics on synthesis of calcium hydroxyapatite by solution combustion route. Bull. Mater. Sci. **33**(1), 7–16 (2010)
45. Coutinho, J.P., Silva, M.C., Meneghetti, S.M.P., Leal, E., de Melo Costa, A.C.F., de Freitas, N.L.: Combustion synthesis of $ZnAl_2O_4$ catalyst using glycine as fuel for the esterification and transesterification of soybean oil: influence the form of heating. Mater. Sci. Forum **727–728**, 1323–1328 (2012)
46. Reinoso, D.M., Fernandez, M.B., Damiani, D.E., Tonetto, G.M.: Study of zinc hydroxy acetate as catalyst in the esterification reaction of fatty acids. Int. J. Low-Carbon Technol. **7**(4), 348–356 (2012)
47. Ropero-Vega, J.L., Aldana-Pérez, A., Gómez, R., Niño-Gómez, M.E.: Sulfated titania [TiO_2/SO_4^{2-}]: a very active solid acid catalyst for the esterification of free fatty acids with ethanol. Appl. Catal. A **379**(1–2), 24–29 (2010)
48. Sheikh, R., Choi, M.-S., Im, J.-S., Park, Y.-H.: Study on the solid acid catalysts in biodiesel production from high acid value oil. J. Ind. Eng. Chem. **19**(4), 1413–1419 (2013)
49. Huang, C.-C., Yang, C.-J., Gao, P.-J., Wang, N.-C., Chen, C.-L., Chang, J.-S.: Characterization of an alkaline earth metal-doped solid superacid and its activity for the esterification of oleic acid with methanol. Green Chem. **17**(6), 3609–3620 (2015)